Hindawi
Mathematical Problems in Engineering
Volume 2018, Article ID 1423613, 17 pages
https://doi.org/10.1155/2018/1423613

Research Article

Dynamic Model and Mechanical Properties of the Two Parallel-Connected CRLD Bolts Verified with the Impact Tensile Test

Liangjun Hao,[1,2] Weili Gong,[1,2] Manchao He,[1,2] Yanqi Song,[1,2] and Jiong Wang[1,2]

[1]*State Key Laboratory for Geomechanics and Deep Underground Engineering, Beijing 100083, China*
[2]*School of Mechanics and Civil Engineering, China University of Mining & Technology, Beijing 100083, China*

Correspondence should be addressed to Weili Gong; weiligongcumtb@163.com

Received 1 June 2018; Accepted 3 September 2018; Published 4 October 2018

Academic Editor: Mijia Yang

Copyright © 2018 Liangjun Hao et al. This is an open access article distributed under the Creative Commons Attribution License, which permits unrestricted use, distribution, and reproduction in any medium, provided the original work is properly cited.

Dynamic model was theoretically established for the two parallel-connected constant-resistance-large-deformation (CRLD) bolts, and the theoretical results were experimentally verified with impact tensile tests on the CRLD bolts samples. The dynamic responses of the double CRLD bolts were investigated under the impact loads with different intensities. The theoretical analyses showed that (1) under relatively small loading the CRLD bolts deform elastically and the deformation finally returns to zero and (2) under the high impact load, including the stable impact load and unstable impact load, the CRLD bolts export structural deformation after the initial elastic deformation. The deformation of the bolts eventually stabilizes at a certain amount of the elongation caused by the relative sliding of the sleeves and rebars. The essential difference between the stable impact load and unstable impact load is that, under the stable impact load, no structural deformation will occur after the impact load ends; under the unstable impact load, the structural deformation will still occur after the impact load ends. The obtained results are of theoretical implications for rock support design with CRLD bolts under the dynamical loading condition.

1. Introduction

With the increasing mining depths for both coal mines and metal ore, tunnels being built in deep ground are often subjected to high stresses and complex geological conditions. Accordingly, surrounding rock masses in deep ground tend to experience various static and dynamic disasters such as creep and rock bursts [1–4]. The constant-resistance-large-deformation bolt possesses more excellent performance than the traditional rebar in the areas of the control of roadway with slow and large deformation, the prevention of dynamic disaster in deep mine, and the monitoring and early warning of landslide [5]. So far, there has been no a dynamic model for the double CRLD bolts acting in parallel, which can be used to explain the dynamic impact test results and recognize the dynamic response characteristics and furthermore provides guidance in the security and stability of the roadway support.

Over years, various ground support techniques and bolt structures have been developed for support and retention of the newly exposed face surrounding the excavation in deep mines. Compared to the traditional strength bolt and yieldable bolt, the energy-absorbing bolt has both the strength of the former bolt and the deformation capacity of the latter one [6]. The energy-absorbing bolts that can meet the said requirement include the Garford Solid Dynamic Bolt [7, 8], Roffex [8], energy-absorbing rock bolt [9], cone bolt [10–12], MCB cone bolt (modified cone bolt with elongation as much as 180 mm) [13, 14], and D bolt with large load-bearing and deformation (elongation as long as 400 mm) [6]. In order to adapt to the increasing demands for the support system and bolt device in deep underground engineering, a novel bolt possessing ultrahigh energy-absorbing capacity by deforming with an extraordinarily large elongation at high constant resistance was developed by Manchao He, known as the constant-resistance and large-deformation bolt (CRLD bolt in 2011) [15].

At present, the research progress on CRLD bolts mainly focuses on three aspects. (1) Theoretically, the constitutive

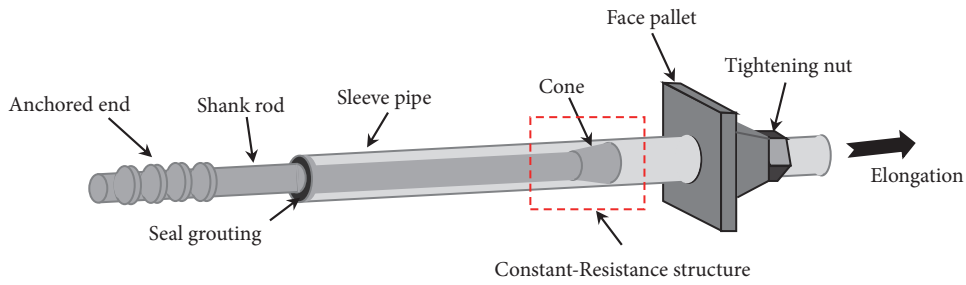

Figure 1: Schematic of the three-dimensional view for the CRLD bolt.

equation of the CRLD bolt under gradual loading is established, which proves the characteristics of constant resistance and large deformation of CRLD bolt [16]. (2) In terms of experimental studies, the CRLD bolt/cable static tensile tests verify the static constitutive equation [17] and in addition the CRLD bolt dynamic tensile tests embody the energy-absorbing and anti-impacting performances and CRLD structural feature [18–21]. (3) In the project, the CRLD bolts are mainly used for the control of slow and large deformation of deep soft rock roadway [5, 22, 23], roadway effective support under rock burst coal bump [2, 4–6, 9], and the monitoring and advance warning of the landslide in opencast mine [24, 25]. So far, there has been no a theoretically dynamic model of the double CRLD bolts acting in parallel for investigating the corresponding properties, except for experimental and engineering analysis [16].

In order to guide the support of the surrounding rock mass under the dynamic disasters in deep underground excavation, the theoretical model for the double CRLD bolts acting in parallel under impact load is established according to the working principle and the impact tensile test of the double CRLD bolts support. After verifying the correctness and stability of the theoretical model through experimental data, the dynamic response characteristics for the double CRLD bolts under the impact load with different intensities are further discussed.

2. Impact Tensile Test

2.1. Working Principle for Double CRLD Bolts Support. Figure 1 shows schematically the structure of the CRLD bolt which is actually a compound device consisting of the following elements: a piston-like cone body installed on a bolt shank (a rebar); a sleeve pipe with its inner diameter slightly smaller than the diameter of the large-end diameter of the cone; a face pallet and a tightening nut functioning as the retention elements. The anchored end of the shank bar is bonded by means of grout. When the axial external load (pull load) is applied on the far end (the face pallet end) of the bolt in the direction opposite to the anchored end, the sleeve pipe will displace in the same direction relative to the cone which is actually the elongation of the CRLD bolt. The motion of the sleeve is equivalent to the displacement of the cone relative to the internal surface of the elastically deformable sleeve pipe. The small-end diameter of the cone is designed to be a little smaller than the internal diameter of the sleeve in order to allow for the easy fitting of the cone body into the pipe. The large-end diameter of the cone is slightly larger than the inner diameter of the sleeve pipe in order to generate the frictional resistance (i.e., the working resistance of the CRLD bolt) during the relative sliding between the cone and sleeve pipe. The elastic limit of the shank bar is more than the frictional resistance. Thus the shank only deforms elastically when the bolt is subjected to the external load.

Figure 2 demonstrates the working principle of the double CRLD bolts acting in parallel in stabilizing the surrounding rock mass. It is considered that the double CRLD bolts are equivalent with the same geometric parameters and material parameters and maintain simultaneous deformation during the support process. The anchored end is fixed inside the stable interior region by resin or cement grouts and the sleeve is located in the unstable surface region. The face pallet is in close contact with the free surface of the surrounding rock mass and plays a supporting role on the roadway. During the dilation of the surrounding rock mass, the bolts system will restrain the dilation so that a tensile load is induced at the face pallet end.

In the initial support process, the pull force exerted by the pallet and nut on the sleeve pipe does not reach the constant resistance force P_{cr} which is the maximum static friction; when the cone slides inside the sleeve pipe, the sleeve pipe, being relatively static with the cone in the direction opposite to anchored end of the bar, only exports elastic elongations of the shank rod as shown in Figure 2(a). If the pull force exerted by the pallet and nut on the sleeve pipe exceeds the constant resistance force P_{cr}, the sleeve pipe will be displaced in the direction opposite to anchored end of the bar, exporting elongations with structural deformation as shown in Figure 2(b).

2.2. Testing System and Results. Figure 3 illustrates the impact tensile test system of the double CRLD bolts acting in parallel (i.e., modified SHTB test system developed at State Key Laboratory for Geomechanics and Deep Underground Engineering in China University of Mining & Technology Beijing), which is specially used to explore the dynamic characteristics of the double bolts acting in parallel under impact load. The double CRLD bolts impact tensile test system is mainly divided into three parts: Hopkinson dynamic loading system (Figure 3(a)(i)), double bolts impact tensile system (Figure 3(a)(ii)), and data acquisition system (Figure 3(a)(iii)).

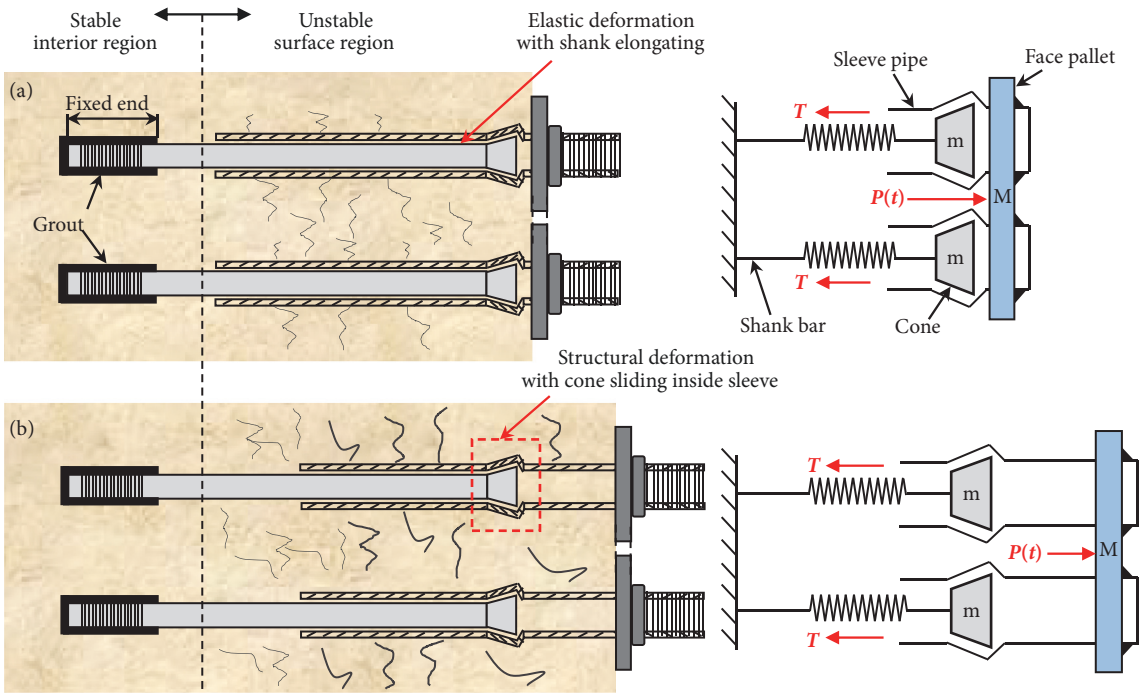

Figure 2: Working principle of the double CRLD bolts acting in parallel in stabilizing the surrounding rock mass: (a) initial support with elastic deformation of the double bolts and (b) late support with structural deformation of the double bolts.

Table 1: Material parameters of the CRLD bolt samples for experiment.

	Rod and cone	Sleeve	Pallet
Material	#45 steel	#20 Ti steel	Steel
Mass (Kg)	3.26	1.24	33.2
Elastic modulus (GPa)	210	206	210
Poisson's ratio	0.269	0.3	0.3

Specifically the Hopkinson dynamic loading system contains the following sections: a loading system being able to provide pressure range between 0 and 25 MPa (Figure 3(b)(i)), a guidance system with length 3950 mm (Figure 3(b)(ii)), and a bullet made of #35 CrMn steel (length L is 800 mm, diameter is 75 mm, and quality is 27.6Kg) as shown in Figure 3(b)(iii). In detail double bolts impact tensile system consists of the following elements: an impact rod whose diameter is equal to that of the bullet (length is 1500 mm, quality is 51.7Kg, density is 7800 Kg/m^3, and elastic stress wave velocity is 5190 m/s), two guide frames with the goal of supporting the impact rod coaxial with the loading system, and a fixed bearing functioning to fix the anchored ends of the double CRLD bolts (the guide frames and fixed bearing are all made of high-strength cast steel), two equivalent CRLD bolts samples with the same geometric parameters and material parameters (the parameters are presented in Figure 4 and Table 1), the face pallet being able to slide freely in the horizontal direction and involving three force sensors to measure impact load when impact rod is hit, and the tightening nut fixing the face pallet over the sleeve. Figure 3(b)(iv, viii) shows the double CRLD bolts impact tensile system from different perspectives. The data acquisition system includes speed monitor measuring the velocity of the bullet rushing out of the bore (Figure 3(b)(v)), load monitor real-time displaying impact load exerted by the impact rod on the face pallet (Figure 3(b)(vi)), and displacement monitor capturing the elongation of sleeve tail end in time (Figure 3(b)(vii)).

Figure 3(c) demonstrates the schematic view of the impact tensile test of the double CRLD bolts acting in parallel in the vertical direction which is more convenient to understand the experimental process. After the erection of all the experimental apparatus is completed, loading controller sets the barometric pressure, and simultaneously the speed, load, and displacement monitor are ready to start sampling. The pressure released by air cylinder pushes forward the bullet to do accelerated movement in the bore. The high-speed bullet that rushes out of the bore strikes the impact rod whose opposite end intimately contacts the face pallet, so the double CRLD bolts whose sleeve pipes are bonded to the face pallet in parallel by their nuts produce the corresponding mechanical behavior. During this process speed monitor records the velocity at which the bullet hits the impact rod, load monitor real-time records and images the load on the face pallet through the force sensors, and simultaneously displacement

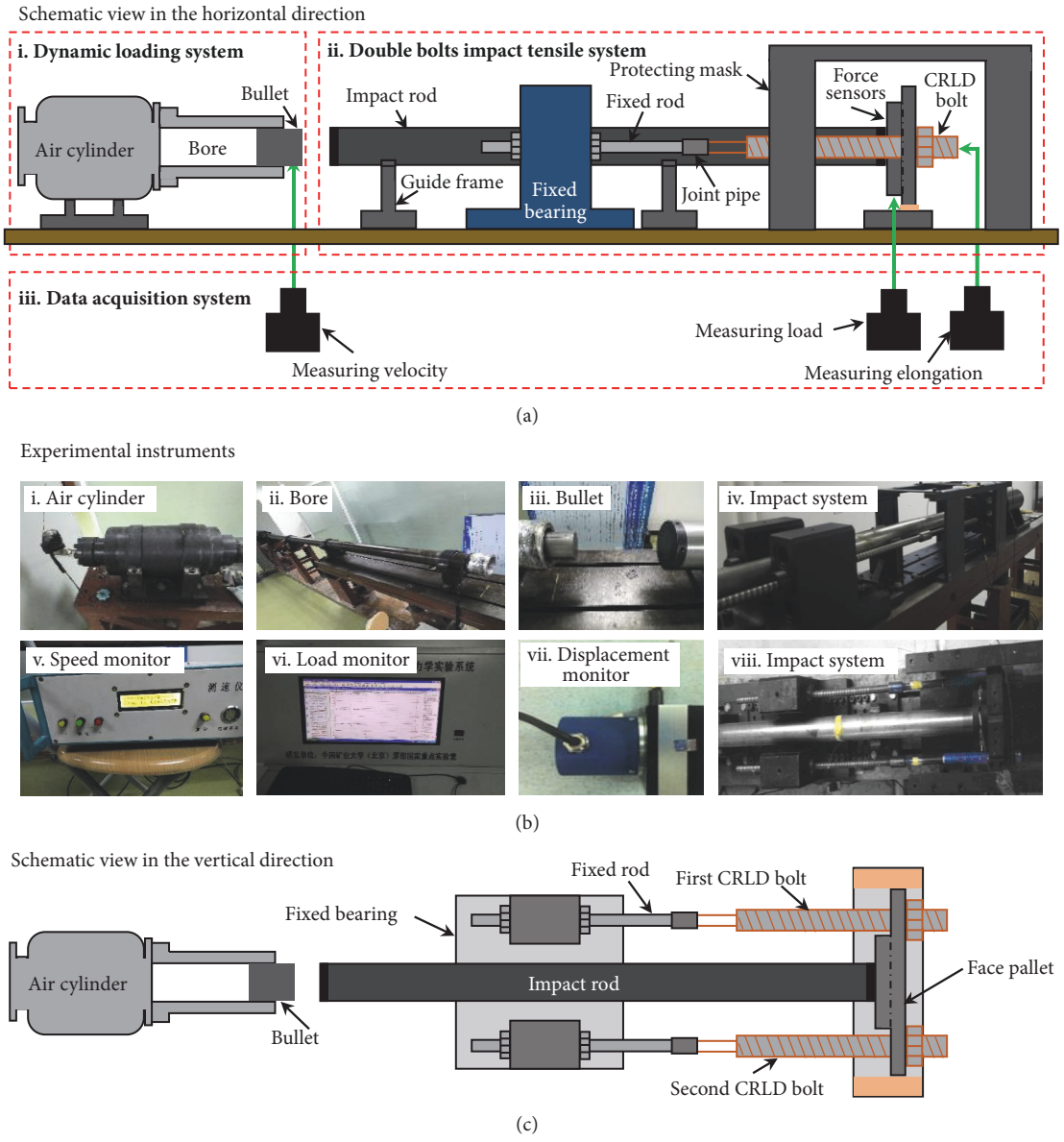

Figure 3: Experimental setup for the impact tensile test of the double CRLD bolts: (a) schematic view in the horizontal direction; (b) experimental instruments; and (c) schematic view in the vertical direction.

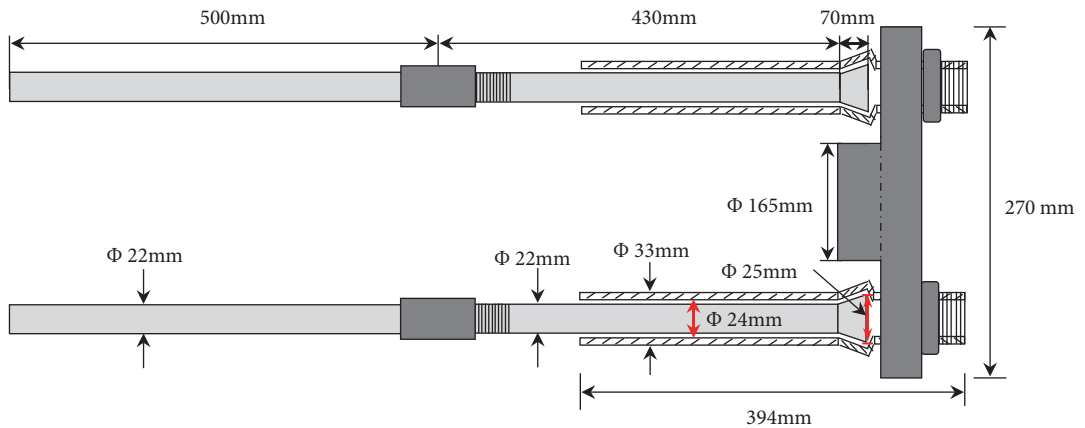

Figure 4: Geometric parameters of the double CRLD bolts samples for experiment.

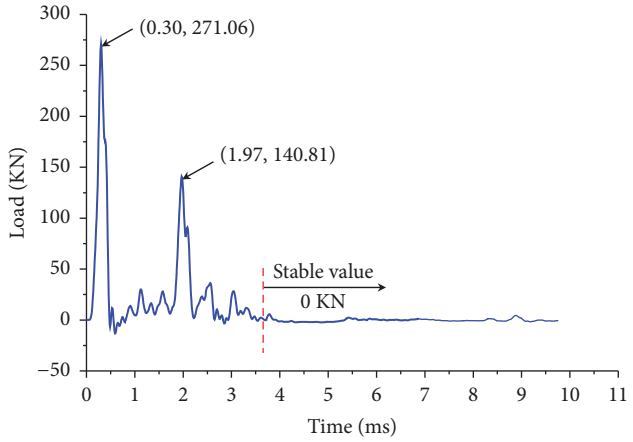

FIGURE 5: Impact load-time curve for double CRLD bolts samples acting in parallel. (The gas pressure is 1.0MPa and the speed of the bullet is 6.14m/s.)

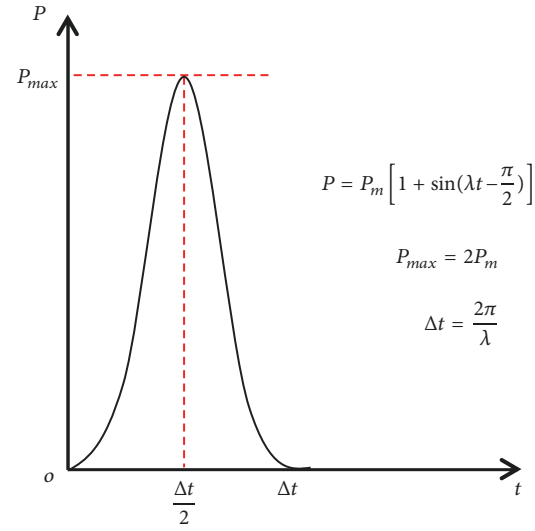

FIGURE 6: The curve of impact load over time (P_{max} and Δt are the intensity and duration of impact load, respectively).

monitor remembers and displays the elongation of the double bolts tails.

Figure 5 shows the experimental impact load-time curve for the double CRLD bolts samples in parallel. Intensity of air source is applied at 1.0MPa and the strike speed of the bullet is measured as 6.14m/s. It can be seen that the load drastically attains the maximum value 271.06KN at a moment 0.30ms in the time axis and sharply drops to the stable value immediately. Interestingly, the load reaches a second peak value 140.81KN when at 1.97ms.

3. Dynamic Model for Double CRLD Bolts Acting in Parallel

The impact load is simulated by a trigonometric function for its mechanical properties of rapid rise and fall in a very short period of time, and it can be expressed by

$$P(t) = P_m\left[1 + \sin\left(\lambda t - \frac{\pi}{2}\right)\right] \quad (1)$$

where P_m and λ determine the intensity and duration of impact load, respectively. Specifically, the intensity of impact load (denoted by P_{max}) is $P_{max} = 2P_m$, and the duration of impact load (denoted by Δt) is $\Delta t = 2\pi/\lambda$. It can be seen that the impact load achieves the maximum value at the time of π/λ from the curve of impact load as shown in Figure 6.

When the intensity of impact load varies, the force condition and motion situation of the CRLD bolts have great difference. Hence, the impact load is divided into three types in accordance with the different intensities. (i) For the elastic impact load, the CRLD bolts only deform elastically during the entire process. (ii) For the stable impact load, the structural deformation of the CRLD bolts is generated; that is, the sleeve slides relatively to the cone. Notably, the relative slippage has stopped when the impact load ends. (iii) For unstable impact load, the CRLD bolts also produce structural deformation, but the relative sliding will continue after the impact load is over. The force and deformation of the CRLD bolts under the three kinds of impact load are discussed, and the mechanical properties are further studied.

Figure 7 clearly explains the mechanical model of the double CRLD bolts acting in parallel under the elastic impact load. The sleeve and the shank rod always have no relative sliding, and only the shank rod is elastically elongated and compressed. The motion of the double CRLD bolts consists of two processes: the combined action of the impact load and the internal force of the shank (see Figure 7(a)); then the internal force of the shank alone (see Figure 7(b)). The bolts are in a state of rest at the initial moment, and the impact load begins to act on the face pallet, as shown in Figure 7(a). Under the impact load and the internal force of the shank, the double bolts elastically deform, as shown in Figure 7(b). After the impact load is complete, the bolts oscillate elastically only under the shank force, as shown in Figure 7(c).

The impact load $P(t)$ is exerted on the face pallet along the direction of movement (i.e., $t \leq \Delta t$), and the internal forces $2kx$ (k is the stiffness of the single shank) of the double shank rods are applied in the opposite direction of motion, as shown in Figure 7(b). The displacement of the double bolts, starting with the initial rest position, is represented by x. A force balance on the double bolts gives

$$(M + 2m)\ddot{x} = P(t) - 2kx \quad (2)$$

where m is the mass of the shank and cone for the single CRLD bolt and M is the mass of the face pallet and double sleeves. The overdot denotes differentiation with respect to the time, t.

Substituting (1) into (2) then can be rewritten into a standard form of second-order ordinary nonhomogeneous differential equation.

$$(M + 2m)\ddot{x} + 2kx = P_m \sin\left(\lambda t - \frac{\pi}{2}\right) + P_m \quad (3)$$

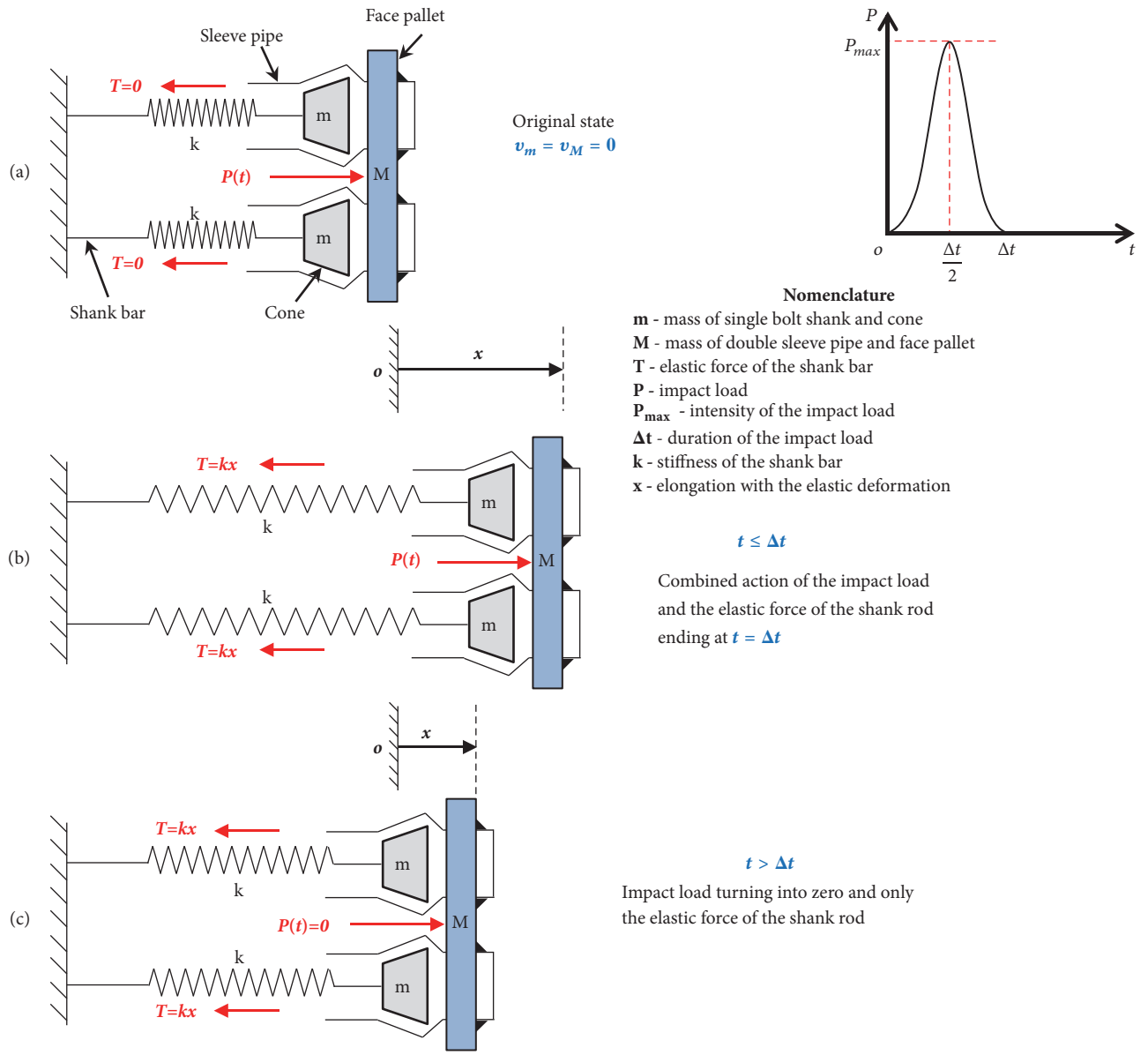

FIGURE 7: Mechanical model of double CRLD bolts under the elastic impact load: (a) original state of the double bolts; (b) combined action of the impact load and the elastic force of the shank bar; and (c) only the elastic force of the shank bar.

The solution to (3), with the introduction of two free variables C_1 and C_2, is

$$x = C_1 \sin(\hat{\omega} t) + C_2 \cos(\hat{\omega} t) + \frac{P_m}{2k - (M + 2m)\lambda^2} \sin\left(\lambda t - \frac{\pi}{2}\right) + \frac{P_m}{2k} \quad (4)$$

$$\dot{x} = C_1 \hat{\omega} \cos(\hat{\omega} t) - C_2 \hat{\omega} \sin(\hat{\omega} t) + \frac{P_m \lambda}{2k - (M + 2m)\lambda^2} \cos\left(\lambda t - \frac{\pi}{2}\right) \quad (5)$$

where

$$\hat{\omega} = \sqrt{\frac{2k}{M + 2m}}. \quad (6)$$

For the initial conditions $x = \dot{x} = 0$ when $t = 0$, the two free variables can be given by the following.

$$C_1 = 0$$
$$C_2 = \frac{P_m}{2k - (M + 2m)\lambda^2} - \frac{P_m}{2k} \quad (7)$$

At the time of impact load ending, that is, t = Δt, the displacement and velocity of the bolts, respectively, become $x_{\Delta t} = x(\Delta t)$ and $\dot{x}_{\Delta t} = \dot{x}(\Delta t)$.

After the impact load is completed (i.e., t > Δt), the bolts continue to elastically deform under the internal forces of the

shanks as shown in Figure 7(c). Another force balance gives the following.

$$(M + 2m)\,\ddot{x} = -2kx \tag{8}$$

The solution to (8), with the two free variables C_3 and C_4, is as follows.

$$x = C_3 \sin\left[\widehat{\omega}\,(t - \Delta t)\right] + C_4 \cos\left[\widehat{\omega}\,(t - \Delta t)\right] \tag{9}$$

$$\dot{x} = C_3\widehat{\omega} \cos\left[\widehat{\omega}\,(t - \Delta t)\right] - C_4\widehat{\omega} \sin\left[\widehat{\omega}\,(t - \Delta t)\right] \tag{10}$$

Substituting the continuity conditions $x = x_{\Delta t}$ and $\dot{x} = \dot{x}_{\Delta t}$ when $t = \Delta t$ into (9) and (10), then the two free variables can be given by the following.

$$\begin{aligned} C_3 &= \frac{\dot{x}_{\Delta t}}{\widehat{\omega}} \\ C_4 &= x_{\Delta t} \end{aligned} \tag{11}$$

Figure 8 clearly explains the mechanical model of the double CRLD bolts acting in parallel under the stable impact load. The double CRLD bolts not only generate elastic deformation but also cause structural deformation. The sleeve pipes slide with respect to the cones, and the relative sliding has stopped when the impact load ends. The situation of force and motion for the double CRLD bolts can be divided into four processes under the stable impact load: the elastic deformation (Figure 8(b)); the structural deformation (Figure 8(c)); the elastic recovery under the impact load and shank force (Figure 8(d)); and the elastic recovery under only the shank force (Figure 8(e)).

At the initial moment, the double bolts are at a state of rest and the impact load begins to act on the face pallet, as shown in Figure 8(a). The double bolts deform elastically under the impact load and shank force, as shown in Figure 8(b). Once the amount of the deformation exceeds the maximum elastic deformation of the CRLD bolt, implying that the internal force of the shank exceeds the constant resistance of the CRLD bolt, the double bolts start to undergo structural deformation. The sleeves and the cones slide relative to each other. The sleeves continue to move forward under the impact load and sliding friction, while the cones oscillate back and forth under the shank force and sliding friction, as shown in Figure 8(c). The speed of the sleeves gradually decreases since the impact load on the sleeves gradually decreases at a later stage and the sliding friction remains unchanged. When the speed of the sleeve pipes is reduced to zero, the relative sliding is completed. At this moment, the impact load continues to work. The double CRLD bolts produce elastic elongation and compression under the impact load and shank force until the end of the impact load, as shown in Figure 8(d). After the impact load is over, the bolts continue to deform elastically under the internal force of the shank along, as shown in Figure 8(e).

In the initially elastic deformation stage (i.e., $x \le x_{cr}$, and x_{cr} is the amount of maximum elastic deformation of the CRLD bolt corresponding to the constant resistance), as shown in Figure 8(b), the double bolts elastically deform under the impact load and the shank force. Therefore, the force balance equation is equivalent to (2), and the displacement-time relationship and velocity-time relationship of the bolts in initially elastic stage under stable impact load are (4) and (5), respectively.

Under the elastic impact load, the bolts do not reach the maximum elastic deformation during the whole impact process. Different from the elastic impact load, the bolts reach the amount x_{cr} of maximum elastic deformation at the end of the initial phase under the stable impact load. It can be seen that the end time of the initial phase (denoted by t_1) satisfies $x(t_1) = x_1 = x_{cr}$. The maximum elastic deformation is given by (for details see [16])

$$x_{cr} = \frac{P_{cr}}{k} \tag{12}$$

$$P_{cr} = 2\pi I_s I_c f \tag{13}$$

where P_{cr} is the constant resistance of the CRLD bolt, I_s is the sleeve elastic constant, I_c is the cone geometrical constant, and f is the coefficient of the static friction.

After the initial phase is completed, the speed of sleeve and shank becomes as follows.

$$\begin{aligned} \dot{x}_1 &= \dot{x}\left(t_1\right) \\ &= \left[\frac{P_m}{2k} - \frac{P_m}{2k - (M + 2m)\,\lambda^2}\right]\widehat{\omega} \sin\left(\widehat{\omega} t_1\right) \\ &\quad + \frac{P_m \lambda}{2k - (M + 2m)\,\lambda^2} \cos\left(\lambda t_1 - \frac{\pi}{2}\right) \end{aligned} \tag{14}$$

Once the bolts deform beyond the maximum elastic deformation, implying that the internal force in the shank rod exceeds the constant resistance, the bolts begin to produce structural deformation by the relative sliding of the sleeve and shank, as shown in Figure 8(c). The force condition and movement situation become different as the sleeve and shank are no longer relatively stationary. For the sleeves and face pallet, the impact load is exerted in the direction of movement and the sliding friction is applied in the opposite direction, satisfying the equation

$$M\ddot{x} = P\left(t\right) - 2F_d \tag{15}$$

where F_d is the sliding friction force between the shank and sleeve and given by (for details see [16])

$$F_d = 2\pi I_s I_c f_d \tag{16}$$

where f_d is the coefficient of dynamic friction between them. Solving (15), we can get the displacement-time relationship and speed-time relationship of the bolts in the structural deformation stage under stable impact load:

$$x = -\frac{P_m}{M\lambda^2} \sin\left(\lambda t - \frac{\pi}{2}\right) + \frac{P_m - 2F_d}{2M} t^2 + C_5 t + C_6 \tag{17}$$

$$\dot{x} = -\frac{P_m}{M\lambda} \cos\left(\lambda t - \frac{\pi}{2}\right) + \frac{P_m - 2F_d}{M} t + C_5 \tag{18}$$

where C_5 and C_6 are two free variables. Substituting the continuity conditions $x = x_1$ and $\dot{x} = \dot{x}_1$ when $t = t_1$ into

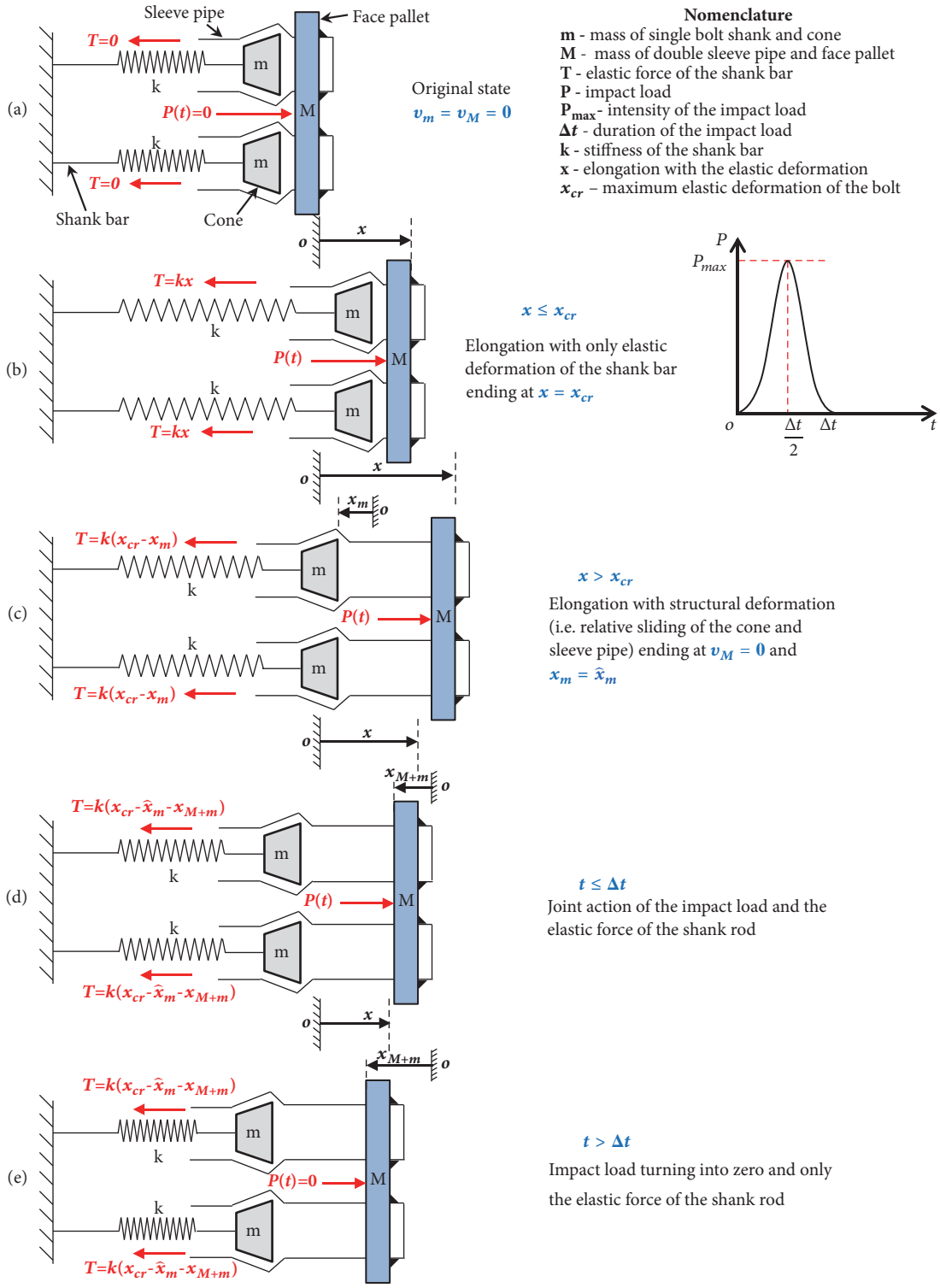

Figure 8: Mechanical model of double CRLD bolts under the stable impact load: (a) original state of the double bolts; (b) initially elastic deformation stage; (c) structural deformation stage; (d) late elastic oscillation stage under the combined action of the impact load and the elastic force of the shank bar; and (e) late elastic oscillation stage only under the elastic force of the shank bar.

(17) and (18), then the two free variables can be obtained as follows.

$$C_5 = \dot{x}_1 + \frac{P_m}{M\lambda}\cos\left(\lambda t_1 - \frac{\pi}{2}\right) - \frac{P_m - 2F_d}{M}t_1$$
$$C_6 = x_1 + \frac{P_m}{M\lambda^2}\sin\left(\lambda t_1 - \frac{\pi}{2}\right) - \frac{P_m - 2F_d}{2M}t_1^2 - C_5 t_1 \quad (19)$$

When the velocity of the sleeves is reduced to zero, the sleeves and the shanks stop sliding relative to each other, and the bolts no longer produce structural deformation. It can be seen that the end time of the structural deformation phase, denoted by t_2, satisfies $\dot{x}(t_2) = 0$. At this time, the displacement of the sleeves and face pallet, denoted by x_2, becomes $x_2 = x(t_2)$.

On the other hand, the shanks and cones oscillate back and forth under the shank forces and sliding friction during the structural deformation phase. The force balance on the cones gives

$$m\ddot{x}_m = k\left(x_1 - x_m\right) - F_d \quad (20)$$

where x_m is the displacement of the cones during the structural deformation stage starting from the end of the initial elastic phase. Substituting (12), (13), and (16) into (20), then we can have the following.

$$m\ddot{x}_m + kx_m = 2\pi I_s I_c\left(f - f_d\right) \quad (21)$$

It is convenient to use the elapsed time τ since the initial movement of the cones and shanks as the independent variable; that is, $\tau = t - t_1$, so the solution to (21) is

$$x_m = C_7\sin(\omega\tau) + C_8\cos(\omega\tau) + \frac{2\pi I_s I_c\left(f - f_d\right)}{k} \quad (22)$$

$$\dot{x}_m = C_7\omega\cos(\omega\tau) - C_8\omega\sin(\omega\tau) \quad (23)$$

where C_7 and C_8 are two free variables and $\omega = \sqrt{k/m}$. Substituting the initial conditions $x_m = 0$ and $\dot{x}_m = \dot{x}_1$ when $\tau = 0$ into (22) and (23), then the two free variables can be given by the following.

$$C_7 = \frac{\dot{x}_1}{\omega}$$
$$C_8 = -\frac{2\pi I_s I_c\left(f - f_d\right)}{k} \quad (24)$$

Substitute $\tau = t - t_1$ into (22) and (23); then the expression of the displacement of the cone with respect to the variable t will be

$$x_m = \frac{\dot{x}_1}{\omega}\sin\left[\omega\left(t - t_1\right)\right] - \frac{2\pi I_s I_c\left(f - f_d\right)}{k}\cos\left[\omega\left(t - t_1\right)\right] + \frac{2\pi I_s I_c\left(f - f_d\right)}{k} \quad (25)$$

and the relationship between the velocity of the cone and the time t will be as follows.

$$\dot{x}_m = \dot{x}_1\cos\left[\omega\left(t - t_1\right)\right] + \frac{2\pi\omega I_s I_c\left(f - f_d\right)}{k}\sin\left[\omega\left(t - t_1\right)\right] \quad (26)$$

At the end time of the structural deformation, the displacement of the cone (denoted by $\hat{x}_m$) becomes

$$\hat{x}_m = x_m\left(t_2\right) \quad (27)$$

and the speed of the cone (denoted by v_m) changes into the following.

$$v_m = \dot{x}_m\left(t_2\right) \quad (28)$$

When the speed of the sleeves is reduced to zero, the sleeves and shanks stop sliding relative to each other and begin to move together. According to the law of conservation of momentum, the common velocity (denoted by v_{M+m}) of them satisfies the following.

$$2mv_m = (M + 2m)\,v_{M+m} \quad (29)$$

The solution to (29) is as follows.

$$v_{M+m} = \frac{2m}{M + 2m}v_m \quad (30)$$

Under the stable impact load, the impact load still exists at the end of the structural deformation of the bolts; that is, $t_2 \le \Delta t$. The double CRLD bolts oscillate elastically under the impact load and shank force, as shown in Figure 8(d). Let x_{M+m} denote the common displacement of the sleeves and shanks during the elastic oscillation starting from the end of the structural deformation. The force balance gives

$$(M + 2m)\,\ddot{x}_{M+m} = 2k\left(x_1 - \hat{x}_m - x_{M+m}\right) - P(t) \quad (31)$$

Substituting (1) into (31), it can be rewritten into a standard form of second-order ordinary nonhomogeneous differential equation.

$$(M + 2m)\,\ddot{x}_{M+m} + 2kx_{M+m} = 2k\left(x_1 - \hat{x}_m\right) - P_m\left[1 + \sin\left(\lambda t - \frac{\pi}{2}\right)\right] \quad (32)$$

Solving (32), we can obtain the displacement-time relationship and speed-time relationship of the bolts during the elastic oscillation under the impact load and shank force

$$x_{M+m} = C_9\sin\left[\widehat{\omega}\left(t - t_2\right)\right] + C_{10}\cos\left[\widehat{\omega}\left(t - t_2\right)\right] + \frac{P_m}{(M + 2m)\,\lambda^2 - 2k}\sin\left(\lambda t - \frac{\pi}{2}\right) + \frac{2k\left(x_1 - \hat{x}_m\right) - P_m}{2k} \quad (33)$$

$$\dot{x}_{M+m} = C_9\widehat{\omega}\cos\left[\widehat{\omega}\left(t - t_2\right)\right] - C_{10}\widehat{\omega}\sin\left[\widehat{\omega}\left(t - t_2\right)\right] + \frac{P_m\lambda}{(M + 2m)\,\lambda^2 - 2k}\cos\left(\lambda t - \frac{\pi}{2}\right) \quad (34)$$

where C_9 and C_{10} are two free variables. Substituting the continuity conditions $x_{M+m} = 0$ and $\dot{x}_{M+m} = v_{M+m}$ when $t = t_2$ into (33) and (34), then the two free variables can be obtained by the following.

$$\begin{aligned} C_9 &= \frac{1}{\widehat{\omega}}\left[v_{M+m} - \frac{P_m\lambda}{(M+2m)\lambda^2 - 2k}\cos\left(\lambda t_2 - \frac{\pi}{2}\right)\right] \\ C_{10} &= -\frac{P_m}{(M+2m)\lambda^2 - 2k}\sin\left(\lambda t_2 - \frac{\pi}{2}\right) \\ &\quad - \frac{2k\left(x_1 - \widehat{x}_m\right) - P_m}{2k} \end{aligned} \tag{35}$$

When the impact load is over ($t = \Delta t$), the common displacement of the sleeves and the shanks becomes

$$x_{\Delta t}^{M+m} = x_{M+m}(\Delta t) \tag{36}$$

and their common velocity turns into the following.

$$\dot{x}_{\Delta t}^{M+m} = \dot{x}_{M+m}(\Delta t) \tag{37}$$

At the subsequent times (i.e., $t > \Delta t$), the sleeves and shanks continue to oscillate elastically only under the internal forces of the shanks, satisfying the following equation.

$$(M+2m)\ddot{x}_{M+m} = 2k\left(x_1 - \widehat{x}_m - x_{M+m}\right) \tag{38}$$

The solution to (38), with two free variables C_{11} and C_{12}, is as follows.

$$\begin{aligned} x_{M+m} &= C_{11}\sin\left[\widehat{\omega}(t-\Delta t)\right] + C_{12}\cos\left[\widehat{\omega}(t-\Delta t)\right] \\ &\quad + \left(x_1 - \widehat{x}_m\right) \end{aligned} \tag{39}$$

$$\dot{x}_{M+m} = C_{11}\widehat{\omega}\cos\left[\widehat{\omega}(t-\Delta t)\right] - C_{12}\widehat{\omega}\sin\left[\widehat{\omega}(t-\Delta t)\right] \tag{40}$$

Substituting the continuity conditions $x_{M+m} = x_{\Delta t}^{M+m}$ and $\dot{x}_{M+m} = \dot{x}_{\Delta t}^{M+m}$ when $t = \Delta t$ into (39) and (40), then the two free variables can be obtained as follows.

$$\begin{aligned} C_{11} &= \frac{\dot{x}_{\Delta t}^{M+m}}{\widehat{\omega}} \\ C_{12} &= x_{\Delta t}^{M+m} - \left(x_1 - \widehat{x}_m\right) \end{aligned} \tag{41}$$

As a further result, the displacement x of the bolts during the elastic oscillation relative to the initial position of the whole process can be given by the following.

$$x = x_2 - x_{M+m} \tag{42}$$

Figure 9 clearly explains the mechanical model of the double CRLD bolts acting in parallel under the unstable impact load. The double bolts also produce structural deformation, and the sleeves and shanks slide relative to each other. However, unlike under the stable impact load, the structural deformation caused by relative sliding continues to occur after the impact load is completed. The situation of force and motion for the double CRLD bolts can also be divided into four processes under the unstable impact load: the elastic deformation (Figure 9(b)); the structural deformation under the impact load and shank forces (Figure 9(c)); the structural deformation under the shank forces alone (Figure 9(d)); and the elastic recovery (Figure 9(e)).

At the initial moment, the double bolts are at a state of rest and the impact load begins to act on the face pallet, as shown in Figure 9(a). The double bolts deform elastically under the impact load and shank forces, as shown in Figure 9(b). Once the amount of the deformation exceeds the maximum elastic deformation of the CRLD bolt, implying that the internal force in the shank exceeds the constant resistance of the CRLD bolt, the double bolts start to undergo structural deformation. The sleeves and the cones slid relative to each other. The sleeves continue to move forward under the impact load and the sliding friction, while the cones oscillate back and forth under the shank forces and the sliding friction, as shown in Figure 9(c). When the impact load is over, the relative movement of the sleeves and cones does not stop, and the structural deformation continues to occur under only the shank forces. The sleeves still move forward under the sliding friction, while the cones still oscillate back and forth, as shown in Figure 9(d). The speed of the sleeve pipes gradually decreases due to the sliding friction. When the speed is reduced to zero, the structural deformation caused by the relative sliding no longer occurs. The sleeves and shanks begin to recover elastically under the internal forces of the shanks, as shown in Figure 9(e).

In the initially elastic deformation stage (i.e., $x \le x_{cr}$), as shown in Figure 9(b), the double bolts elastically deform under the unstable impact load and the shank forces. It is completely equivalent to the initial stage under the stable impact load.

Once the bolts deform beyond the maximum elastic deformation x_{cr}, meaning that the internal force in the shank rod exceeds the constant resistance P_{cr}, the bolts begin to produce structural deformation by the relative sliding of the sleeve and shank (Figure 9(c)). The situation of the force and motion becomes different as the sleeve and shank are no longer relatively stationary. For the sleeves and face pallet, the impact load is exerted in the direction of movement and the sliding friction is applied in the opposite direction. Therefore, the force balance equation is equivalent to (15), and the displacement-time relationship and velocity-time relationship of the bolts in the structural deformation stage under the unstable impact load and shank forces are (17) and (18), respectively.

Under the stable impact load, the structural deformation is completed before the end of the impact load. Differently, under the unstable impact load, the structural deformation continues to occur after the impact load is over. At the time of the impact load ending, i.e., $t = \Delta t$, the displacement of the sleeves and pallet changes into

$$\begin{aligned} x_{\Delta t} &= x(\Delta t) \\ &= \frac{P_m}{M\lambda^2} + \frac{P_m - 2F_d}{2M}\left(\frac{2\pi}{\lambda}\right)^2 + C_5\frac{2\pi}{\lambda} + C_6 \end{aligned} \tag{43}$$

and the velocity of them turns into the following.

$$\dot{x}_{\Delta t} = \dot{x}(\Delta t) = \frac{P_m - 2F_d}{M}\frac{2\pi}{\lambda} + C_5 \tag{44}$$

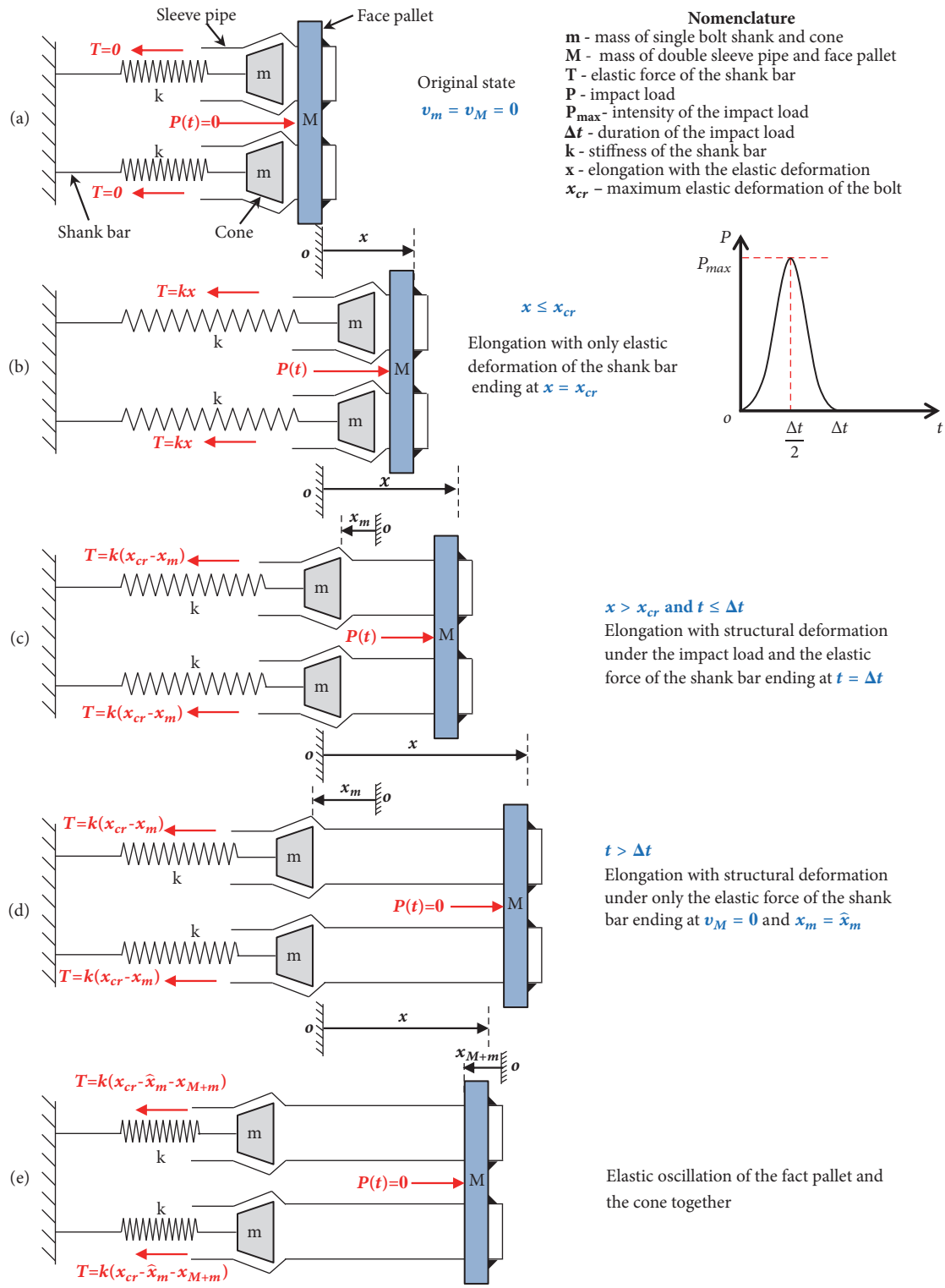

Figure 9: Mechanical model of double CRLD bolts under the unstable impact load: (a) original state of the double bolts; (b) initially elastic deformation stage; (c) structural deformation stage under the combined action of the impact load and the elastic force of the shank rod; (d) structural deformation stage only under the elastic force of the shank bar; and (e) late elastic oscillation stage.

After the impact load is over, i.e., $t > \Delta t$, the sleeves continue to slide forward with respect to the shanks resulting in the structural deformation (Figure 9(d)). At the subsequent times, the sleeves and pallet under only the sliding friction satisfy the following equation.

$$M\ddot{x} = -2F_d \tag{45}$$

Solving (45), we can obtain the displacement-time relationship and speed-time relationship of the sleeves after the impact load ending:

$$x = -\frac{F_d}{M}t^2 + C_{13}t + C_{14} \tag{46}$$

$$\dot{x} = -\frac{2F_d}{M}t + C_{13} \tag{47}$$

where C_{13} and C_{14} are two free variables. Substituting the continuity conditions $x = x_{\Delta t}$ and $\dot{x} = \dot{x}_{\Delta t}$ when $t = \Delta t$ into (46) and (47), then the two variables can be given by the following.

$$\begin{aligned} C_{13} &= \dot{x}_{\Delta t} + \frac{2F_d}{M}\Delta t \\ C_{14} &= x_{\Delta t} + \frac{F_d}{M}\Delta t^2 - C_{13}\Delta t \end{aligned} \tag{48}$$

The velocity of the sleeves gradually decreases due to the sliding friction in the opposite direction of the movement. When the speed is reduced to zero, the sleeves and shanks stop sliding relative to each other, and the bolts no longer produce structural deformation. It can be seen that the end time of the structural deformation, denoted by t_2, satisfies $\dot{x}(t_2) = 0$. At this time, the displacement of the sleeves, denoted by x_2, becomes $x_2 = x(t_2)$.

During the entire process of the structural deformation, including the deformation under the impact load and shank forces (Figure 9(c)) as well as the deformation under only the shank forces (Figure 9(d)), the shanks and cones always oscillate back and forth under the internal forces of the shanks and sliding frictions. It is equivalent to the structural deformation phase under the stable impact load. Similarly, x_m is used to represent the displacement of the cones during the whole process of structural deformation starting from the end of the initial elastic phase, and $\tau = t - t_1$. It can be seen that the displacement of the cones satisfies (20). The displacement x_m and the velocity $\dot{x}_m$ of the cones with respect to the time variable t are, respectively, (25) and (26).

At the end time of the structural deformation caused by the relative sliding of the sleeves and cones, the displacement and velocity of the cones are, respectively, (27) and (28). It needs special attention that $t_2 > \Delta t$ under unstable impact load and $t_2 \leq \Delta t$ under the stable impact load. This is the essential difference between the unstable impact load and stable impact load: under the unstable impact load, the structural deformation will still occur after the impact load ends; under the stable impact load, no structural deformation will occur after the impact load ends.

After the structural deformation of the bolts is completed, the bolts oscillate elastically under only the internal forces of the shank rods (Figure 9(e)). Similarly, let x_{M+m} denote the common displacement of the sleeves and shanks during the elastic oscillation starting from the end of the structural deformation. The force balance of the bolts gives the following.

$$(M + 2m)\,\ddot{x}_{M+m} = 2k\left(x_1 - \hat{x}_m - x_{M+m}\right) \tag{49}$$

Solving (49), we can obtain the displacement-time relationship and speed-time relationship of the bolts during the elastic oscillation under the unstable impact load and shanks forces

$$\begin{aligned} x_{M+m} = {} & C_{15}\sin\left[\hat{\omega}\left(t - t_2\right)\right] + C_{16}\cos\left[\hat{\omega}\left(t - t_2\right)\right] \\ & + \left(x_1 - \hat{x}_m\right) \end{aligned} \tag{50}$$

$$\dot{x}_{M+m} = C_{15}\hat{\omega}\cos\left[\hat{\omega}\left(t - t_2\right)\right] - C_{16}\hat{\omega}\sin\left[\hat{\omega}\left(t - t_2\right)\right] \tag{51}$$

where C_{15} and C_{16} are two free variables. Substituting the continuity conditions $x_{M+m} = 0$ and $\dot{x}_{M+m} = v_{M+m}$ when $t = t_2$ into (50) and (51), then the two variables can be obtained by the following.

$$\begin{aligned} C_{15} &= \frac{v_{M+m}}{\hat{\omega}} \\ C_{16} &= -\left(x_1 - \hat{x}_m\right) \end{aligned} \tag{52}$$

As a further result, the displacement x of the bolts during the elastic oscillation relative to the initial position of the whole process can be given by the following.

$$x = x_2 - x_{M+m} \tag{53}$$

In particular, the second peak in the load-time curve is due to the face pallet hitting the impact rod during the elastic recovery. In the impact tensile test for the double CRLD bolts acting in parallel, the bullet hits the impact rod and the first peak is formed on the face pallet that is in close contact with the impact rod. Subsequently, the CRLD bolts start to move and the impact rod remains approximately stationary. After the deformation of the bolts reaches the maximum value, the bolts recover elastically in the opposite direction. The second peak is generated when pallet hits the impact rod located in initial position again. The intensity of the second pulse is determined by the internal forces of the shanks when the deformation of the bolts reaches the maximum.

Under the elastic impact load, the bolts only deform elastically and the sleeves and shanks are always relatively stationary. When the deformation of the bolts is maximum, the internal forces in the shanks of the double bolts, that is, the intensity of the second pulse, can be given by

$$P_{max2} = 2k \cdot \max(x) \tag{54}$$

where P_{max2} is the intensity of the second pulse load and $\max(x)$ denotes the maximum deformation of the bolts during the whole process.

When the pallet recovers and reaches the initial position, the speed of the bolts attains a minimum value which is

Table 2: Experimental and calculated data under three gas pressures to determine the transmission coefficients.

Gas pressure (MPa)	Bullet velocity (m/s)	Shock wave in impact rod		Shock wave in face pallet		Ratios	
		Duration (ms)	Intensity (KN)	Duration (ms)	Intensity (KN)	K_1	K_2
1.5	10.97	0.31	980.96	0.45	505.58	1.45	0.52
1.8	12.60	0.31	1126.70	0.45	610.89	1.45	0.54
2.0	14.48	0.31	1294.80	0.45	740.69	1.45	0.57

a negative value indicating the maximum speed in reverse. Therefore, the starting time T of the second pulse satisfies

$$\dot{x}(T) = \min(\dot{x}) \tag{55}$$

where T is starting time of the second pulse load and $\min(\dot{x})$ denotes the minimum speed of the bolts during the whole process.

Under the stable impact load and unstable impact load, the bolts produce structural deformation, and the sleeves slide relative to the shanks. When the deformation of the bolts is maximum, the deformation of the shank is $x_{cr} - \hat{x}_m$; hence the intensity of the second pulse load is as follows.

$$P_{max2} = 2k\left(x_{cr} - \hat{x}_m\right) \tag{56}$$

Different from being under the elastic impact load, when the speed of the bolts reaches a minimum value, the bolts only complete the recovery of elastic deformation and the bolts do not return to the initial position due to the presence of structural deformation. At the subsequent times, the pallet continues to move in the maximum speed in reverse until it collides with the impact rod resulting in the second pulse load. The starting time T of the second pulse is

$$T = T_1 + T_2 \tag{57}$$

where T_1 is the time when the speed of the bolts reaches the minimum value, and satisfies $\dot{x}(T_1) = \min(\dot{x})$. T_2 is the time from the bolts speed reaching the minimum value to the pallet hitting the impact rod and satisfies $T_2 = -[\max(x) - x(T_1)]/\min(\dot{x})$.

4. Verification of the Theoretical Results with Impact Tensile Test

In the impact tensile test for the double CRLD bolts acting in parallel, the bullet hits the impact rod and the shock wave is generated in the impact rod. According to the traditional SHPB experimental theory [26, 27], the duration Δt^* of the shock wave in the impact rod can be calculated by

$$\Delta t^* = \frac{2l}{c} \tag{58}$$

where l is the length of the bullet equal to 800 mm and c is the speed of the elastic stress wave in the impact rod equal to 5190 m/s. The intensity P^*_{max} of the shock wave in the impact rod can be given by

$$P^*_{max} = \frac{1}{2}\rho c v s \tag{59}$$

where v is the striking velocity of the bullet equal to 17.94m/s, ρ is the density of the impact rod equal to 7800 kg/m^3, and s is their contact area (i.e., the same cross-sectional area of the bullet and the impact rod) and can be obtained by the following.

$$s = \pi\left(\frac{0.075}{2}\right)^2 \approx 0.00441786\left(m^3\right) \tag{60}$$

When the shock wave in the impact rod propagates to the contact surface with the face pallet, a portion of the energy is projected into the face pallet, so that the double CRLD bolts acting in parallel produce corresponding responses. Let K_1 represent the ratio of the duration Δt of the shock wave in face pallet relative to Δt^*, and let K_2 denote the ratio of the intensity P_{max} of the shock wave in the face pallet relative to P^*_{max}; then we can have the following.

$$\Delta t = K_1 \cdot \Delta t^* \tag{61}$$

$$P_{max} = K_2 \cdot P^*_{max} \tag{62}$$

In order to determine the ratios K_1 and K_2, the impact tensile tests for the double CRLD bolts acting in parallel at the gas pressures of 1.5MPa, 1.8MPa, and 2.0MPa were performed. Monitoring the striking velocities of the bullet at the three different gas pressures, then the durations and the intensities of the shock waves in the impact rod can be calculated by (58) and (59), respectively. Based on the measured durations and intensities of the shock waves in the face pallet, the corresponding K_1 and K_2 can be obtained (the specific data is shown in Table 2).

Taking the average values of K_1 and K_2 as their reference values, and then $K_1 = 1.45$ and $K_2 = 0.54$. From (58) and (61), the duration of the shock wave in face pallet at the 1.0MPa gas pressure can be obtained by the following.

$$\Delta t = 1.45 \times \frac{2 * 0.8}{5190} \approx 0.45 \times 10^{-3}\,(\mathrm{s}) = 0.45\,(\mathrm{ms}) \tag{63}$$

The intensity of the shock wave in the pallet, from (59) and (62), can be obtained by the following.

$$\begin{aligned} P_{max} &= 0.54 \times \frac{1}{2} \times 7800 \times 5190 \times 6.14 \times 0.0044 \\ &\approx 2.9649 \times 10^5\,(\mathrm{N}) = 296.49\,(\mathrm{KN}) \end{aligned} \tag{64}$$

Combined with the other physical parameters of the specimens for CRLD bolts (see Table 3), the theoretical load-time curve for the double CRLD bolts acting in parallel under impact load can be obtained, as shown in Figure 10. The

Table 3: Parameters used in drawing the analytical curve.

Parameter	value
Constant resistance P_{cr} (KN)	184.17
Corresponding displacement on constant resistance x_{cr} (mm)	2.3
Coefficient on intensity of impact load P_m (KN)	148.245
Coefficient on duration of impact load λ (1/ms)	13.96
Mass of single bolt shank and cone m (Kg)	3.26
Mass of double sleeve and pallet M (Kg)	35.68
Stiffness of the shank k (KN/mm)	79.8
Sleeve elastic constant I_s (N/m^3)	1.003×10^{11}
Cone geometrical constant I_c (m^3)	2.902×10^{-6}
Static frictional coefficient f	0.1007
Dynamic frictional coefficient f_d	0.0879

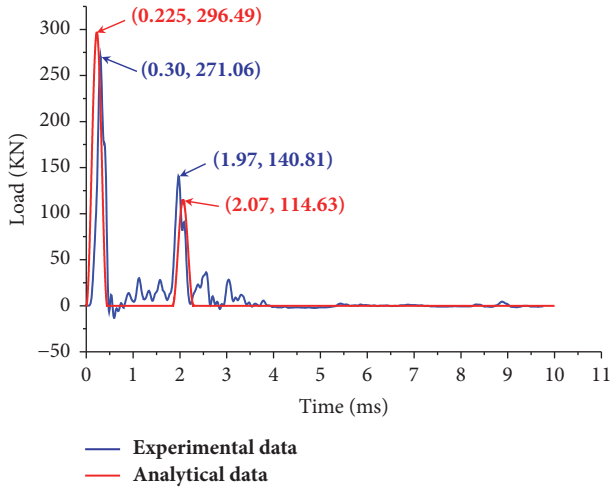

Figure 10: Comparison of experimental data and analytical data about the load of the double CRLD bolts. (The gas pressure is 1.0MPa and the speed of the bullet is 6.14m/s.)

load reaches the maximum value 296.49KN at 0.225ms and attains the second peak value 114.63KN at 2.07ms. From the comparison of the experimental data and the analytical data about the load of the double CRLD bolts, it can be seen that their change trends and the two peak values are basically consistent, which indicate the correctness and reliability of the theoretically dynamic model.

5. Discussion about the Dynamic Responses of the Double CRLD Bolts

In order to investigate the mechanical responses of the double CRLD bolts acting in parallel under impact loads with different intensities and an identical duration (Δt = 2 ms), it is quite necessary to determine the corresponding ranges of the intensities of the three different types of impact load (the specific values as shown in Table 4). Specifically we, respectively, choose one from each of the three types of impact load for comparison and analysis, which possesses the intensities of 100KN, 250KN, and 800KN (see Figures 11, 12, and 13, respectively).

In particular, it has been known that the second pulse in the load-time curve of the CRLD bolts is caused by the experimental equipment. It does not belong to the mechanical properties of the CRLD bolts. Therefore, it is not considered for the second pulse in the following analysis.

Figure 11(a) shows the displacement-time curve and the load-time curve of the CRLD bolts under the impact load with the intensity 100KN and the duration 2 ms. The maximum displacement 1.06mm of the bolts does not reach the maximum elastic displacement 2.3mm, so there is no relative sliding of the sleeves and the shanks, only the elastic tension and compression of the shanks themselves during the entire impact process. Both the load and the displacement of the bolts eventually become zero when the bolts tend to be stable. Figure 11(b) indicates the load-displacement curve of the CRLD bolts under the elastic impact load. The load firstly rises and then decreases with the increase of the displacement. However after the displacement reaches the maximum value, the load begins to reduce with the decrease of the displacement. Furthermore, the time of the displacement reaching its peak significantly lags behind the time of the load achieving its maximum.

Figure 12(a) illustrates the displacement-time curve and the load-time curve of the CRLD bolts under the impact load with the intensity 250KN and the duration 2 ms. The maximum displacement 2.74mm of the CRLD bolts exceeds the maximum elastic displacement 2.3mm, so the bolts produce structural deformation caused by the relative sliding of the sleeves and shanks. Specifically the sleeves and shanks begin to slide relative to each other at 1.31ms when the internal force of the shank reaches the constant resistance 184.17KN as well as with the corresponding displacement 2.3mm. The relative sliding ends at 1.61ms, at which the bolts achieve the maximum displacement. The impact load still continues until it becomes zero at 2 ms. The relative sliding has stopped before the end of the impact load, which indicates the impact being the stable impact load. In addition the displacement finally stabilized at 1.06mm after the oscillation.

Figure 12(b) indicates the load-displacement curve of the CRLD bolts under the stable impact load. The load firstly rises and then decreases with the increase of the displacement. However after the displacement reaches the maximum value, the load begins to reduce with the decrease of the displacement. Furthermore, the time of the displacement reaching its peak significantly lags behind the time of the load achieving its maximum.

Figure 13(a) shows the displacement-time curve and the load-time curve of the CRLD bolts under the impact load with the intensity 800KN and the duration 2 ms. The maximum displacement 31.67mm of the CRLD bolt exceeds the maximum elastic displacement 2.3mm, so the bolts also produce structural deformation caused by the relative sliding of the sleeves and shanks. Specifically the sleeves and shanks start to slide relative to each other at 0.82ms when the internal force of the shank reaches the constant resistance 184.17KN as well as with the corresponding displacement

Table 4: Critical ranges for three different types of impact load.

Type	Load intensities (KN)	Characteristic
Elastic impact load	$P_{max} \leq 218.74$	Only elastic deformations without structural deformations
Stable impact load	$218.75 \leq P_{max} \leq 412.18$	End of structural deformations earlier than end of impact
Unstable impact load	$P_{max} \geq 412.19$	End of structural deformations later than end of impact

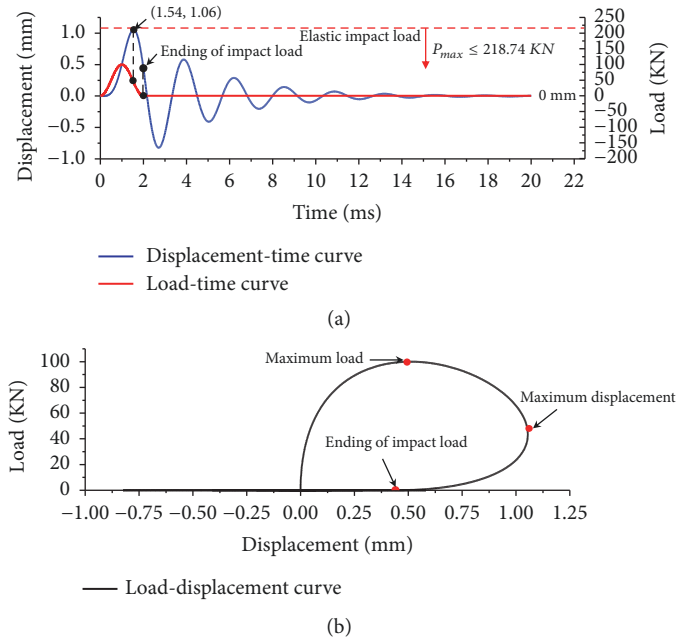

Figure 11: Curves for double CRLD bolts acting in parallel under impact load with intensity 100KN and duration 2 ms: (a) displacement-time curve and Load-time curve and (b) load-displacement curve.

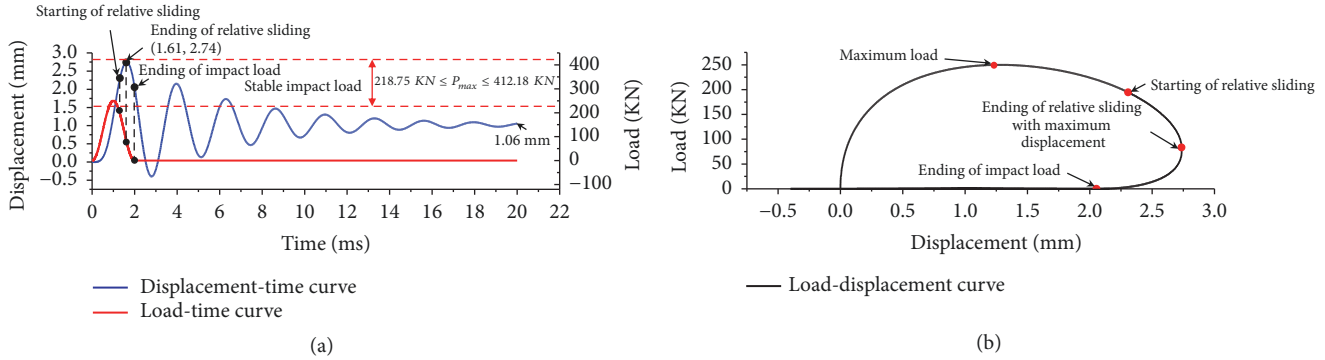

Figure 12: Curves for double CRLD bolts acting in parallel under impact load with intensity 250KN and duration 2 ms: (a) displacement-time curve and Load-time curve and (b) load-displacement curve.

2.3mm. Although the impact load is completed at 2 ms, the relative sliding of the sleeves and shanks does not stop. The relative slippage still continues until 3.06ms, at which the bolts reach the maximum displacement 31.67mm. The relative sliding still takes place after the end of the impact load, which demonstrates the impact being the unstable impact load. In addition the displacement finally stabilized at 28.87mm after the oscillation.

Figure 13(b) indicates the load-displacement curve of the CRLD bolts under the unstable impact load. The load first rapidly rises and then slowly decreases with the increase of the displacement. Interestingly, the displacement continues to increase after the ending of the impact load. Furthermore, the time of the displacement reaching its peak significantly lags behind the time of the load achieving its maximum.

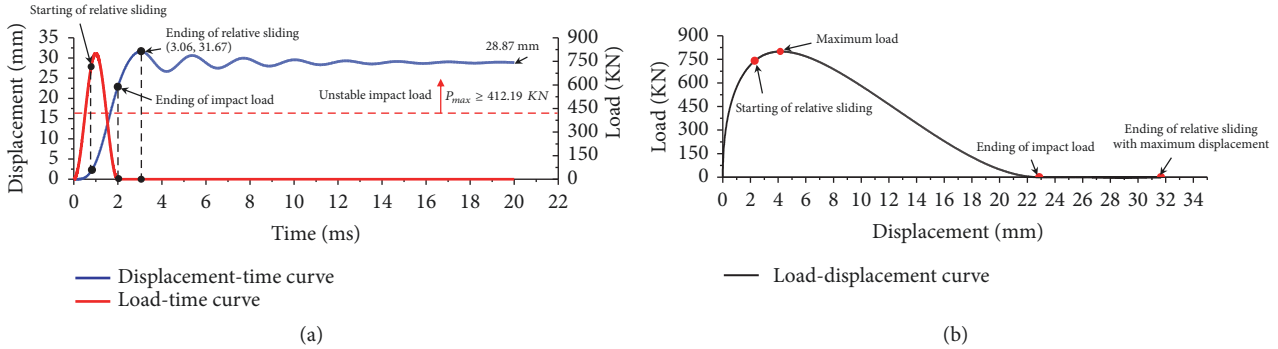

FIGURE 13: Curves for double CRLD bolts acting in parallel under impact load with intensity 800KN and duration 2 ms: (a) displacement-time curve and Load-time curve; and (b) load-displacement curve.

6. Conclusion

Under the impact loads with different intensities, the situations of force and motion for the double CRLD bolts acting in parallel have great difference, which results in the different mechanical responses. (i) Under relatively small loading, the CRLD bolts deform elastically and the deformation finally returns to zero. (ii) Under the high impact load, including the stable impact load and unstable impact load, the CRLD bolts undergo structural deformation after the initial elastic deformation. The deformation of the CRLD bolts eventually stabilizes at a certain amount caused by the relative sliding of the sleeves and shanks. The essential difference between the stable impact load and unstable impact load is that, under the stable impact load, no structural deformation will occur after the impact load ends; under the unstable impact load, the structural deformation will still occur after the impact load ends.

In addition, under the three different impact loads, the time of the displacement reaching its peak significantly lags behind the time of the load achieving its maximum. Under the elastic impact load and stable impact load, there is a contraction of displacement before the end of the load. However, under the unstable impact load, the displacement continues to increase during the entire loading process.

Based on the above discussion about the mechanical response properties of the CRLD bolts under the impact loads with different intensities, some guidance can be provided for the safe and stable support of the roadway with different buried depth and lithology.

Data Availability

The data used to support the findings of this study are available from the corresponding author upon request.

Conflicts of Interest

The authors declare that they have no conflicts of interest.

Acknowledgments

The research work is supported by the Special Funds from the National Natural Science Foundation of China [grant number 51574248]; the National Key Research and Development Program [grant number 2016YFC0600901]; and the Open Foundation of the State Key Laboratory for Geomechanics and Deep Underground Engineering, Beijing [grant number SKLGDUEK1728].

References

[1] W. D. Ortlepp and T. R. Stacey, "Performance of tunnel support under large deformation static and dynamic loading," *Tunnelling and Underground Space Technology*, vol. 13, no. 1, pp. 15–21, 1998.

[2] PK. Kaiser, M. Diederichs, and S. Yazici, "Cable bolt performance during mining induced stress change-three case example," in *Proceedings of the international symposium on rock support*, pp. 331–384, Sudbury, Canada, 1992.

[3] C. Windsor and A. Thompson, "Reinforcement systems mechanics, design, installation, testing, monitoring & modelling," *International Journal of Rock Mechanics and Mining Sciences*, vol. 35, no. 4-5, p. 453, 1998.

[4] M. Cai, "Principles of rock support in burst-prone ground," *Tunnelling and Underground Space Technology*, vol. 36, no. 6, pp. 46–56, 2013.

[5] M. He, C. Li, W. Gong, J. Wang, and Z. Tao, "Support principles of NPR bolts/cables and control techniques of large deformation," *Yanshilixue Yu Gongcheng Xuebao/Chinese Journal of Rock Mechanics and Engineering*, vol. 35, no. 8, pp. 1513–1529, 2016.

[6] C. C. Li, "A new energy-absorbing bolt for rock support in high stress rock masses," *International Journal of Rock Mechanics and Mining Sciences*, vol. 47, no. 3, pp. 396–404, 2010.

[7] R. Varden, R. Lachenicht, A. G. P. Thompson Jr, and E. Villaescusa, "Development and implementation of the Garford Dynamic bolt at the Kanowna Belle mine," in *Proceedings of the 10th Underground operators conference*, pp. 95–104, Launceston, AsuIMM, Melborune, Australia, 2008.

[8] F. Charette and M. Plouffe, "A new rock bolt concept for underground excavations under high stress conditions," in *Proceedings of the Sixth international symposium on ground support in mining and civil engineering construction*, pp. 225-40, SAIMM, Johannesburg, South Africa, 2008.

[9] A. Ansell, "Dynamic testing of steel for a new type of energy absorbing rock bolt," *Journal of Constructional Steel Research*, vol. 62, no. 5, pp. 501–512, 2006.

[10] A. F. Jager, "Two new support units for the control of rockburst damage," *International Journal of Rock Mechanics and Mining Sciences & Geomechanics Abstracts*, vol. 31, no. 2, p. A97, 1994.

[11] L. St-Pierre, F. P. Hassani, P. H. Radziszewski, and J. Ouellet, "Development of a dynamic model for a cone bolt," *International Journal of Rock Mechanics and Mining Sciences*, vol. 46, no. 1, pp. 107–114, 2009.

[12] M. H. Turner and J. R. Player, "Seismicity at big bell mine," in *Proceedings of the Proceedings Massmin*, pp. 791–797, Melbourne, Australia, 2000.

[13] D. Gaudreau, A. Gendron, and J. P. Basque, *Apparatus and Method for A Yieldable Tendon Mine Support US Patent*, vol. 6, 2002.

[14] B. Simser, W. C. Joughin, and W. D. Ortlepp, "The performance of Brunswick mines rockburst support system during a severe seismic episode," *Journal of the Southern African Institute of Mining and Metallurgy (JSAIMM)*, pp. 217–233, 2002.

[15] M. C. He, "Constant-resistance and large-deformation bolt," Chinese patent, 2011, Patent 2011: No. ZL 2010 1 0196197.2, Certificate No. 852069.

[16] M. C. He, W. L. Gong, J. Wang et al., "Development of a novel energy-absorbing bolt with extraordinarily large elongation and constant resistance," *International Journal of Rock Mechanics & Mining Sciences*, vol. 67, pp. 29–42, 2014.

[17] M.-C. He, J. Wang, X.-M. Sun, and X.-J. Yang, "Mechanics characteristics and applications of prevention and control rock bursts of the negative poisson's ratio effect anchor," *Journal of Coal Science & Engineering (China)*, vol. 39, no. 2, pp. 214–221, 2014.

[18] M. He, C. Li, and W. Gong, "Elongation and impacting experimental system for bolts with constant resistance and large deformation and finite element analysis," *Yanshilixue Yu Gongcheng Xuebao/Chinese Journal of Rock Mechanics and Engineering*, vol. 34, no. 11, pp. 2179–2187, 2015.

[19] L. Chen, H. Manchao, and G. Weili, "Analysis on kinetic features of constant resistance high deformed bolt under different impact velocity," *Coal Science and Technology*, vol. 43, no. 9, pp. 53–58, 2015.

[20] C. Li, M.-C. He, and W.-L. Gong, "Analysis on impact dynamics of negative Poisson's ratio effect of anchor bolt with constant resistance and large deformation," *Meitan Xuebao/Journal of the China Coal Society*, vol. 41, no. 6, pp. 1393–1399, 2016.

[21] M. C. He, C. Li, W. L. Gong, L. R. Sousa, and S. L. Li, "Dynamic tests for a Constant-Resistance-Large-Deformation bolt using a modified SHTB system," *Tunnelling and Underground Space Technology*, vol. 64, pp. 103–116, 2017.

[22] M. He and Z. Guo, "Mechanical property and engineering application of anchor bolt with constant resistance and large deformation," *Yanshilixue Yu Gongcheng Xuebao/Chinese Journal of Rock Mechanics and Engineering*, vol. 33, no. 7, pp. 1297–1308, 2014.

[23] X.-J. Yang, J.-W. Pang, B.-T. Zhang et al., "Deformation and failure mechanism and support measures of the soft rock roadway in the air return laneway," *Meitan Xuebao/Journal of the China Coal Society*, vol. 39, no. 6, pp. 1000–1008, 2014.

[24] M. C. He, Z. G. Tao, and W. L. Gong, "Geo-disaster prediction with double-block mechanics based on Newton force measurement," *Geomechanics and Geophysics for Geo-Energy and Geo-Resources*, vol. 3, no. 2, pp. 107–119, 2017.

[25] Z.-G. Tao, H.-P. Li, G.-L. Sun, L.-J. Yin, and X.-L. Zhang, "Development of monitoring and early warning system for landslides based on constant resistance and large deformation anchor cable and its application," *Rock and Soil Mechanics*, vol. 36, no. 10, pp. 3032–3040, 2015.

[26] J. S. Rinehart, *Stress Transients in Solids*, Santa Fe, New Mexico, Mexico, 1975.

[27] W. K. Nowacki, *Stress waves in non-elastic solids*, Pergamon Press, Oxford-New York-Toronto, Ont., 1978.

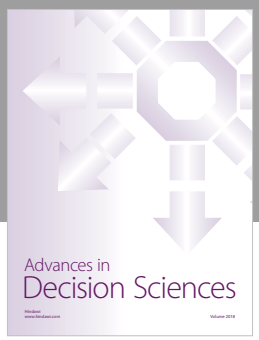

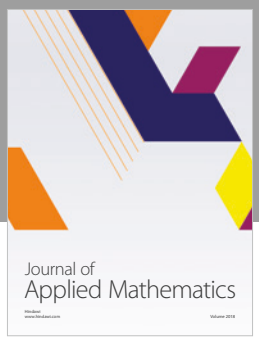

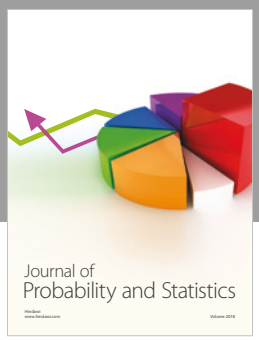

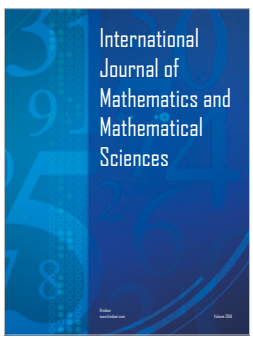

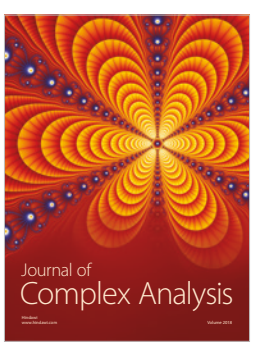

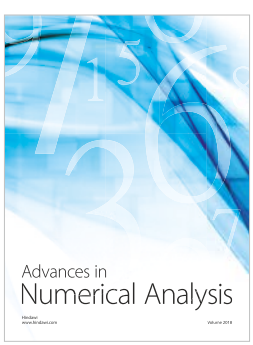

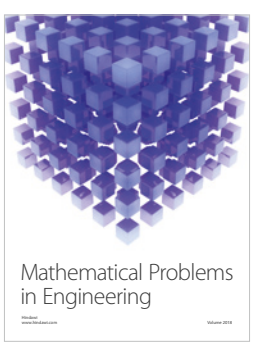

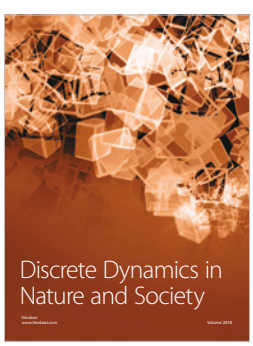

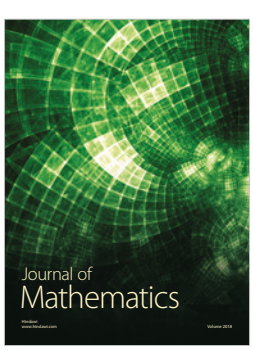

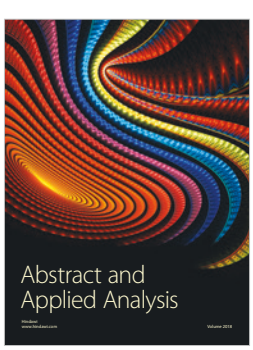

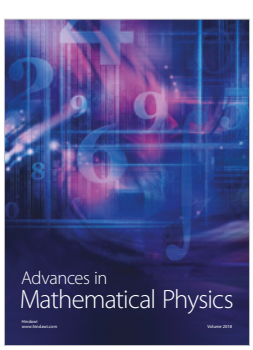

Hindawi

Submit your manuscripts at
www.hindawi.com